Polymer Journal, Vol. 22, No. 9, pp 781—792 (1990)

Investigation of Molecular Motion and Structures of Side Chains in Poly(γ-methyl L-glutamate-*co*-γ-stearyl L-glutamate) by Spin-Probe Technique and ^{13}C Cross-Polarization Magic Angle Spinning Nuclear Magnetic Resonance

Masashi YAMAGUCHI and Akihiro TSUTSUMI

Department of Applied Physics, Faculty of Engineering, Hokkaido University, Sapporo 060, Japan

(Received March 9, 1990)

ABSTRACT: The molecular motion and structure in poly(γ-methyl L-glutamate-*co*-γ-stearyl L-glutamate)s with various molar compositions were investigated by means of spin-probe technique and ^{13}C CP/MAS NMR. By the latter, it was confirmed that a certain part of long alkyl chains forms paraffin-like crystallites as observed in homopolymer of stearyl L-glutamate, and other part exists as the amorphous phase below crystalline melt. An introduction of a small amount of stearyl group considerably raises the mobility of the spin-probe which is embedded in the side chain region surrounding the α-helical main chain, and further increase of stearyl content does not remarkably alter mobility. It is suggested that spin-probes exist in the amorphous region composed of stearyl groups, and mainly reflect the motional state of this region. the difference of the mobility between methyl L-glutamate side chain and stearyl group are also investigated by the scalar decoupled ^{13}C NMR spectra in the solid state.

KEY WORDS Molecular Motion / Poly(L-glutamate) / Long Alkyl Side Chain / Spin-Probe Technique / ^{13}C CP/MAS NMR /

Many studies have been made on side chain motions in α-helical polypeptides, and it has been found that above a certain temperature considerable motion occurs, whereas the α-helical main chain remains rigid.[1-3] Therefore, the physical properties of α-helical poly(glutamate)s in the solid state are closely related to the state of the side chain motion. Recently, Watanabe *et al.*[4-6] reported on poly(glutamate)s having long alkyl side chains ($n \geqq 10$: n is number of alkyl carbon atoms) that side chains form paraffin-like crystallites and at a certain temperature above the crystalline melt, thermotropic liquid crystalline natures appear. These phenomena have not been observed in poly(glutamate)s having short side chains such as poly(γ-methyl L-glutamate). It has been suggested that considerable mobility[4] of the long alkyl side chains surrounding α-helical main chain is important for the formation of such a liquid crystal. However, detailed studies focused on the side chain motion of these polymers have not been carried out. It is of interest to elucidate the particular features of the motion of long side chains in comparison with short side chains.

In this work, we carried out the electron spin resonance (ESR) using spin-probe technique and ^{13}C cross polarization/magic angle spinning nuclear magnetic resonance (CP/MAS NMR) to investigate side chain motion in the copolymers of γ-methyl L-glutamate (short side chain) and γ-stearyl L-glutamate ($n=18$, long side chain) with various molar compositions in the solid state.

It is well known that the spin-probe technique is one of the useful methods to obtain motional information of the host polymers,[7,8]

where a small amount of probes such as nitroxide radicals are dispersed. Especially, for α-helical poly(glutamate), this technique gives us motional information on the side chain region where nitroxide radicals are embedded. On the other hand, ^{13}C CP/MAS NMR allows us to observe each carbon of a molecule separately in the solids state, and therefore gives detailed information on local motion and structure of the side chain.[9-11]

EXPERIMENTAL

Materials

*Poly(*γ-methyl L-glutamate) (PMLG) was kindly supplied by Ajinomoto Co., Ltd. Poly(γ-methyl L-glutamate-*co*-γ-stearyl L-glutamate)s were synthesized by the ester exchange reaction of the PMLG with stearyl alcohol in 1,2-dichloloroethane at 60°C using *p*-toluenesulfonic acid as a catalyst. The degree of substitution of stearyl groups (mol%), D.S., in copolymers was adjusted by changing the alcohol concentration and confirmed by ^1H NMR spectra in the deuterated chloroform–trifuloroacetic acid (80 : 20 wt%) solution. All the samples examined here were films prepared by casting the chloroform solution at room temperature. Abbreviations for the samples are listed in Table I.

For the spin-probe method, two kinds of probes with different sizes were employed, the one is 2,2,6,6-tetramethyl-4-hydroxypiperidine-1-oxyl (TEMPOL) and the other, methyl 12-doxyl-stearate (DOX) as shown Figure 1. The films were immersed in ethanol solution containing 10^{-3} ($mol\,l^{-1}$) probes for 12 h and dried *in vacuo*.

Measurements

ESR spectra were taken with a JEOL X-band (9.2 GHz) spectrometer (JES-FE1X) at the micro wave power 1 mW. The amplitude of the 100 kHz field modulation was 0.3—0.63 Gauss. The temperature was varied from −130 to 150°C. ^{13}C CP/MAS NMR spectra were obtained by a Bruker MSL-400 spectrometer (100 MHz) with the MAS rate of 4 kHz. The acquisition was performed under dipolar decoupling (62.5 kHz). Repetition time was 5.0 s. ^{13}C chemical shifts were calibrated through external glycine (amide carbon 176.03 ppm relative to TMS). ^{13}C NMR spectra under the low power scalar decoupling were measured by a Bruker AM-500 spectrometer (125 MHz). DSC measurements were performed at a scanning rate of 5°C/min in a heating process using a Ringaku-Denki DSC calorimeter.

Table I. Abbriviations of samples and endothermic peak temperatures (T_m) in DSC thermogram

Abbreviation	Stearyl/ml%	T_m/°C
ST83	83%	60
ST62	62%	40
ST38	38%	14
ST25	25%	−20
ST0(PMLG)	0%	Not observed

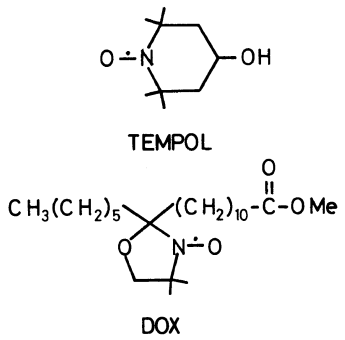

Figure 1. Structures of nitroxide radicals.

RESULTS AND DISCUSSION

Figure 2 shows the ESR spectra of TEMPOL in ST0(PMLG) and ST62 at various temperatures. Below room temperature, the spectra are composed of broad and asymmetric lines in both samples. The values of outer extrema separation, ΔW, were very close to the rigid limit value, indicating the spin-probe motion is almost frozen in the time scale of the

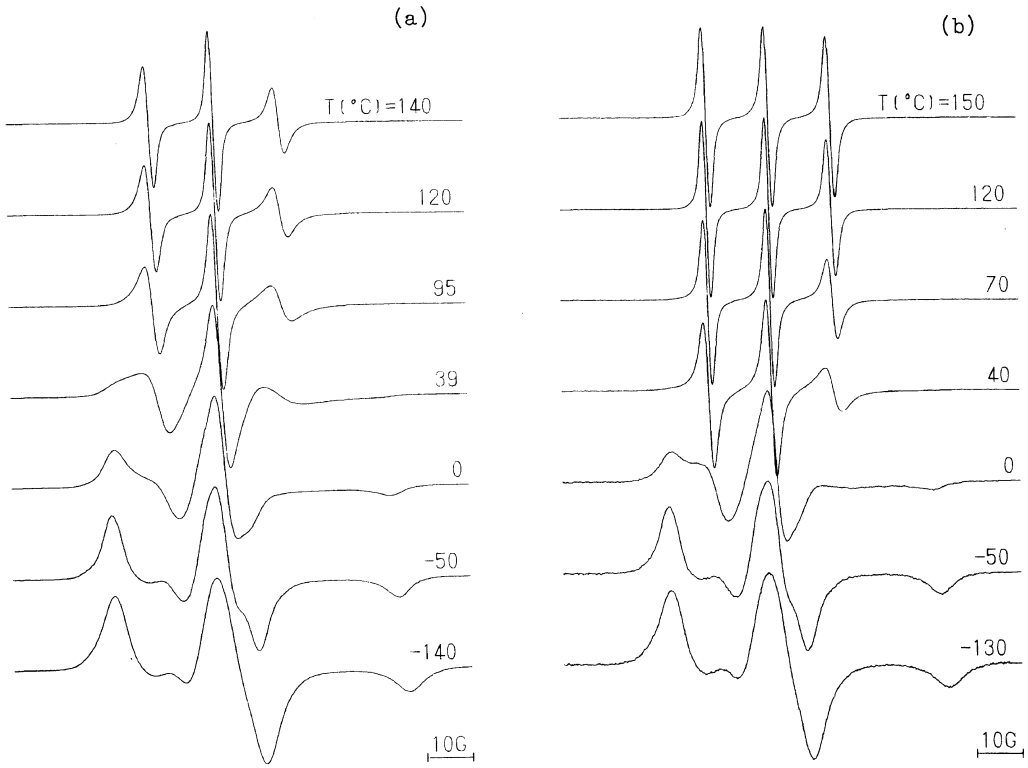

Figure 2. ESR spectra of TEMPOL in ST0 (a) and ST62 (b) at various temperature.

ESR measurement. As the temperature is raised, the line shape becomes slightly sharper and ΔW decreases due to the onset of the spin-probes motion. The spectral line shapes below -50°C are similar in the two samples, indicating the spin-probe in similar motional state. Qualitatively similar spectra are obtained for other copolymers below room temperature.

In the higher temperature region, the spectra show sharp triplet pattern, which is characteristic of rapidly tumbling nitroxide spin-probes. It is well known that the side chain of α-helical ST0(PMLG) undergoes considerably rapid motion at the higher temperature region.[2,3] The sharper spectra of ST62 than that of ST0 (compare the spectra at 120°C for example) further suggests that the side chain mobility of the copolymer is much higher than that of ST0 as in the liquid state.[7]

Figure 3 shows the temperature dependence

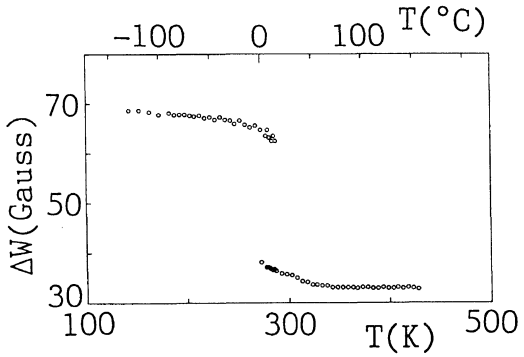

Figure 3. Temperature dependence of ΔW for TEMPOL in ST62.

of ΔW for TEMPOL in ST62. An abrupt decrease occurs in the vicinity of room temperature. Around this temperature, two components, narrow and broad, are plotted, since spectra show complex patterns with subsplitting in high field and low field peaks

due to the partial averaging of the anisotropic hyperfine and Zeeman interactions. Qualitatively similar profiles of ΔW *vs.* T(K) curve are obtained for other samples, though narrowing temperatures differ from each other.

It is usual to define the characteristic narrowing temperature as T_{50G}[12] where ΔW acrosses the value of 50 Gauss.* At T_{50G}, the rotational correlation time of spin-probe, τ_c, has the value of 10^{-8} s for the nitroxide radical, since narrowing occurs when τ_c exceeds the splitting due to hyperfine interactions, ω_{hfs} (in angular frequency unit), $\omega_{hfs}\tau_c \sim 1$. In Figure 4, T_{50G} is plotted as a function of D.S. (degree of substitution of stearyl groups). The higher T_{50G} for DOX than TEMPOL may be attributed to the difference in the probe size, since two probes have a molecular volume of 176 A^3 and 425 A^3 for TEMPOL and for DOX, respectively.[13] Kusumoto *et al.*[12] assumed that the spin-probe in amorphous polymers above the glass transition temperature moves by jump diffusion into neighboring cavities (free volume) produced by segmental motion, and explained the probe dependence of T_{50G} in terms of the critical size of cavities. Since a large cavity is necessary for a large probe, T_{50G} shifts to the higher temperature until the cavity has a critical volume due to the thermal expansion. It has been reported that the side chains of α-helical ST0 do not have a fixed conformation and compose an amorphous like phase.[2,3] The motion of whole side chains causes properties similar to amorphous polymers, indicating that Kusumoto's concept is applicable to the spin-probe motion in the side chain of poly(glutamate).

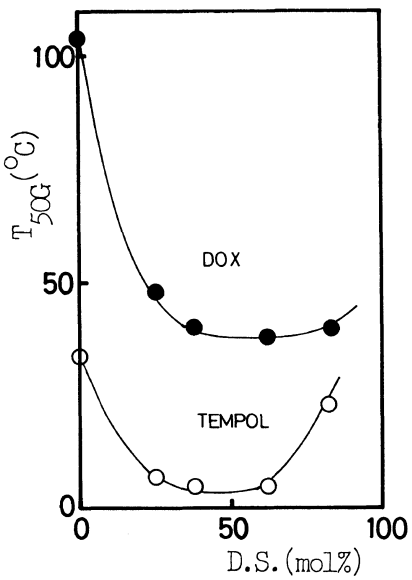

Figure 4. T_{50G} *vs.* D.S.: TEMPOL (○); DOX (●).

Introduction of a small amount of stearyl group considerably lowers the T_{50G} compared to that of ST0 (D.S. = 0%), indicating the high increase of the spin probe motion. In the intermediate region of D.S. = 25—62%, T_{50G} keeps almost a constant value. However, in ST83 (D.S. = 83%), T_{50G} rises again for TEMPOL but not for DOX. These behaviors will be discussed below on the basis of more detailed analysis of the motional state.

The rotational correlation time τ_c of a nitroxide spin-probe which undergoes a fast motion ($10^{-11} < \tau_c < 10^{-9}$), was estimated by the procedures of Freed *et al.*,[7,14] in which the anisotropic rotational motion is taken into account. The line width of ESR spectra is expressed as follows.

$$1/T_2(M) = A + BM + CM^2 \tag{1}$$

where M is the projection quantumn number of ^{14}N spin. A, B, and C are given by

$$A = (2/15)(\omega_0^2/g^2)\{(F_g^0)^2\tau_0 + 2(F_g^2)^2\tau_2\} + (I(I+1)/20)\{(F_A^0)^2\tau_0 + 2(F_A^2)^2\tau_2\} \tag{2}$$

$$B = (4/15)(\omega_0/g)\{F_g^0 F_A^0 \tau_0 + 2F_g^2 F_A^2 \tau_2\} \tag{3}$$

$$C = (1/12)\{(F_A^0)^2\tau_0 + 2(F_A^2)^2\tau_2\} \tag{4}$$

* To avoid ambiguity in determining T_{50G} from $\Delta W - T$(K) curve, the temperature at which the intensities of two subsplitting in the high field line give equal peak intensities was used, in this work. It has been reported that this temperature is very close to T_{50G}.[12] Therefore, the former is abbreviated as T_{50G}, hereafter.

$$F_A^0=(2/3)^{1/2}\{A_z-(1/2)(A_x+A_y)\}$$
$$F_g^0=(2/3)^{1/2}\{g_x-(1/2)(g_x+g_y)\} \quad (5)$$
$$F_A^2=(1/2)(A_x-A_y)$$
$$F_g^2=(1/2)(g_x-g_y)$$

Experimentally, $T_2(M)$ $(M=-1, 0, 1)$ are obtained from the peak height in the first derivative spectra, I_M, for low, central, and high field lines as $T_2(M)=(4\pi/3\sqrt{3})^{1/2} I_M^{1/2}$, respectively.

$$1/\tau_m=6^*D_\perp+m^2(D_\parallel-D_\perp) \quad (m=0, 2) \quad (6)$$

$D_\parallel$ and $D_\perp$ are rotational diffusion coefficients about the major and minor axes of the axially symmetric rotor, respectively. Rotational correlation times $\tau_\parallel$ and $\tau_\perp$ are defined as $(6D_\parallel)^{-1}$ and $(6D_\perp)^{-1}$. Components of A- and g-tensors (A_i, g_i where $i=x, y, z$) refer to the coordinate system fixed to axially symmetric rotor. The major axis is taken to be parallel to the Y-axis of the coordinate fixed to the nitroxide radical whose definition is given elsewhere, where A- and g-tensors are diagonalized.[15] It has been reported that the average correlation times $\tau_c=\sqrt{\tau_\parallel\tau_\perp}$ have similar values to that based on the isotropic rotational model.[16] Therefore, we call hereafter τ_c the isotropic correlation time. For the slow tumbling region $10^{-9}<\tau_c<10^{-7}$, the relation derived from the simulated spectra by Freed *et al.* was used.[17]

$$\tau_c=a(1-S)^b \quad \text{where} \quad S=A_z/A_{z\,\text{rigid}} \quad (7)$$

A_z is the half width of extrema separation and $A_{z\,\text{rigid}}$ is its rigid-limit value. a and b are constants depending on the motional model and intrinsic line width. In this work, the Brownian motion model with an intrinsic line width of 3 Gauss was adopted.

Temperature dependences of τ_c for TEMPOL and DOX in copolymers are shown in Figures 5 and 6, respectively. Both probes do not show a simple linear $\log\tau_c-1000/T$ relationshiop over the whole temperature range, but at least more than two processes exist. The side chains of poly(glutamate)s undergo a small amplitude local motion in the low temperature region, and a large scale motion which is similar to the micro Brownian motion caused by the glass transition in amorphous polymer in the vicinity of the room temperature as described above.[18-20] Kusumoto[12] reported that at a lower temperature than the glass transition, a spin-probe is trapped in a small cavity and undergoes small amplitude rotational oscillation with low activation energy. This process may correspond to the lower temperature process in Figures 5 and 6 (process I). The spin-probe is under the influence of small amplitude local motion of the side chain. On the other hand, it is pointed out that τ_c in this process has a strong dependence on the molecular size and shape of spin-probe. Furthermore, τ_c estimated using eq. 7 depends on the motional mode and intrinsic line width in the calculation. Detailed information about such effects at low temperature may be obtained by spectral simulation according to Freed *et al.*[21] However, such analysis is beyond this work, and therefore further discussion is not given here.

The spin-probe motion above room temperature (process II) is considered to reflect the large scale motion of the side chain, since for ST0(PMLG) and some polypeptides, the correlation frequency (inverse of τ_c) *vs.* $1000/T$(K) curve locates around the extension of this motional process as measured by mechanical, dielectric and NMR relaxation. A small deviation from the extension curve of other experimental methods has been explained by differences in the size of the spin-probe and segment (modified Kusumoto's theory[22]) and the effects of the probe shape.[22] Above 333 K ($1000/T(\text{K})\leqq 3.0$), ST0 has a much longer τ_c than copolymers which give one order smaller τ_c. It is clearly shown here that the side chain region surrounding the helical main chain is highly mobile with the introduction of long alkyl side chains.

The third process (process III) is seen for TEMPOL in the higher temperature region.

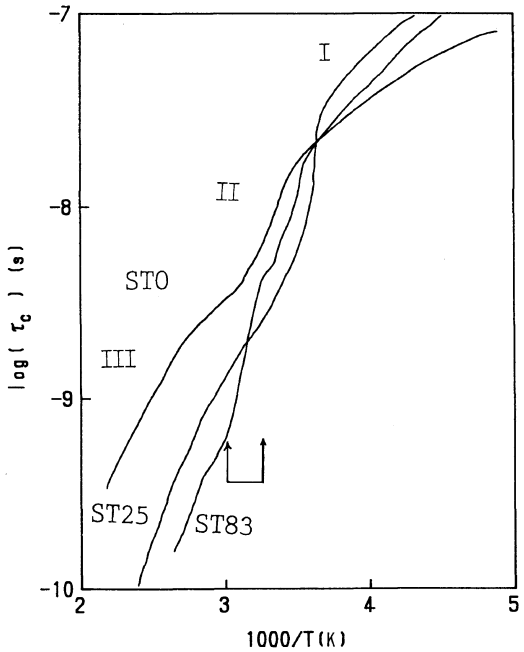

Figure 5. Temperature dependence of τ_c for TEMPOL.

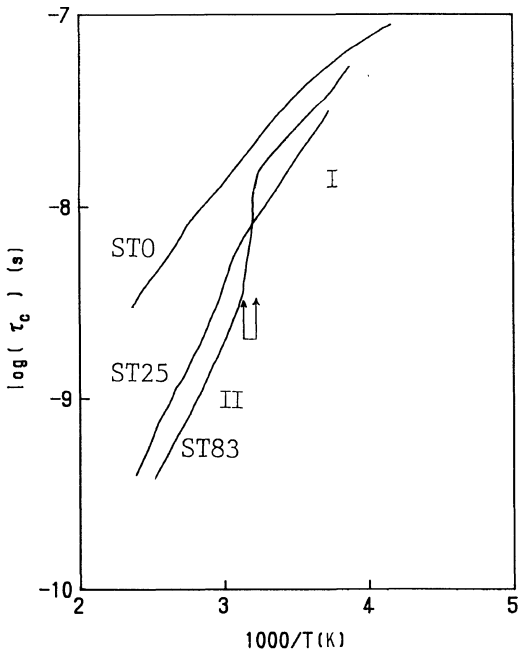

Figure 6. Temperature dependence of τ_c for DOX.

This process may correspond to the motional process involving main chains reported for other polymers.[23]

For ST83, τ_c shows a peculiar temperature dependence superposed on the room temperature process (process II). At around 333 K ($1000/T(\mathrm{K}) \sim 3.0$), τ_c decreases suddenly from a rather large value to the shortest among these copolymers. This occurs in almost the same temperature range, as indicated by two arrows in Figures 5 and 6, for both probes in spite of having very different probe sizes and shapes. This temperature range is close to the endothermic peak in DSC thermogram as seen below, indicating that such a decrease occurs due to melting of the side chain crystalline.

On the basis of these results, more detailed consideration on the above mentioned T_{50G} for ST83 is given as follows. The melting point is close to T_{50G} for DOX, but lower than T_{50G} for TEMPOL. This indicates that the structural state at T_{50G} of ST83 is different for each probe case. In other samples, the peculiar behavior as in ST83 does not occur, since T_{50G} values for both probes are higher than the melting points.

To investigate the anisotropic motion of TEMPOL in the side chain region, anisotropic correlation times $\tau_{\parallel}$ and $\tau_{\perp}$, as estimated by the method described above, are plotted in Figure 7. ST0 has larger values than the copolymers. $\tau_{\perp}$ of ST0 is about 10 times as large as $\tau_{\parallel}$ even at the highest temperature of this measurement, indicating a higher degree of anisotropy. For copolymers, the anisotropy is relatively smaller, and almost vanishes in the high temperature region. $\tau_{\perp}$ decreases with increasing D.S. while $\tau_{\parallel}$ does not show clear D.S. dependence, indicating that the motional state of side chain region in copolymers is reflected more strongly in $\tau_{\perp}$ than in $\tau_{\parallel}$, since the rotation about the minor axis needs more space than that about the major axis to move and is more influenced by the motional state of host polymer. TEMPOL has a relatively spherical shape and undergoes almost isotropic motion in the isotropic liquid. The present results indicate that at the higher temperature,

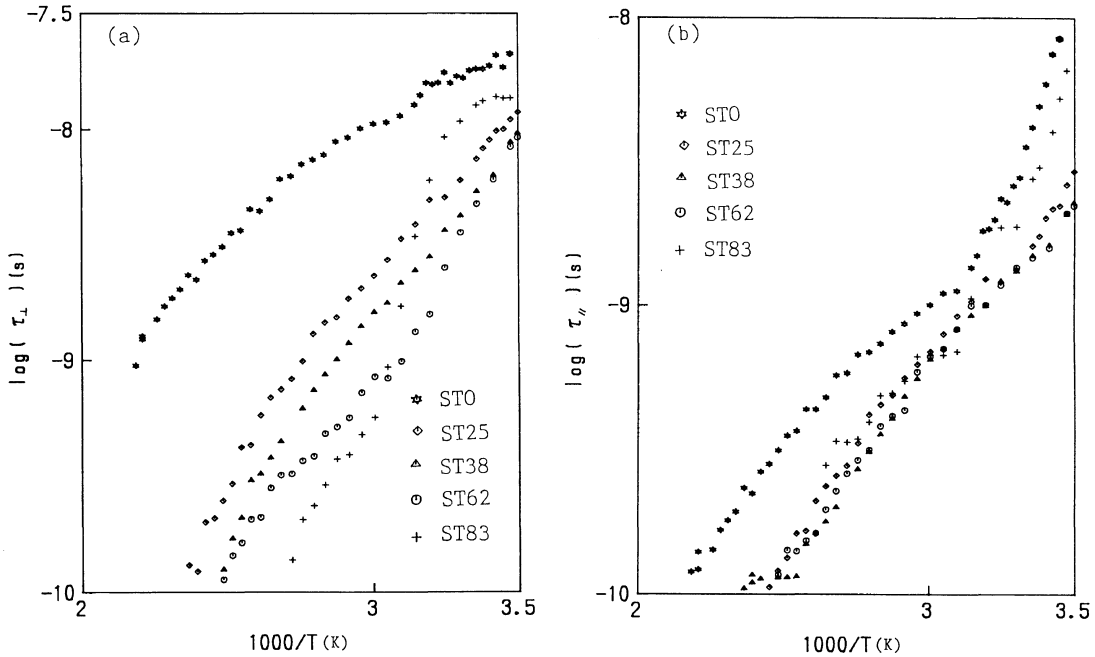

Figure 7. Temperature dependence of anisotropic rotational correlation times for TEMPOL (a) $\tau_{\perp}$ (b) $\tau_{\parallel}$.

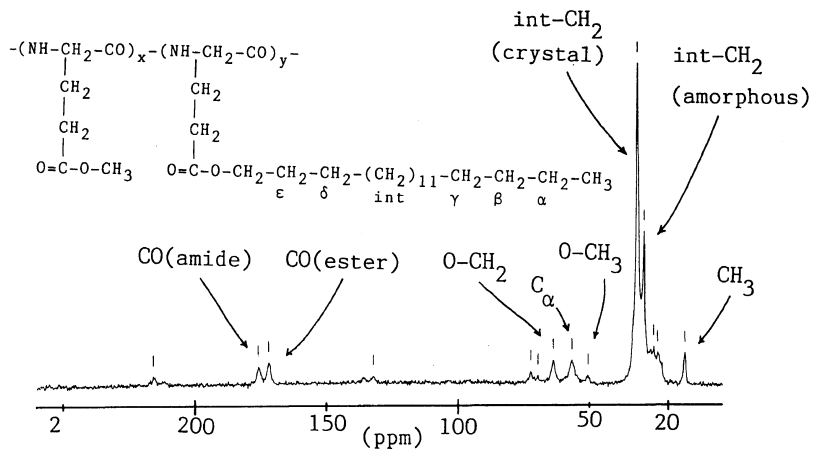

Figure 8. ^{13}C CP/MAS spectrum of ST83 at 40°C.

the motion of side chains in the copolymers is highly isotropic as in the isotropic liquid considerably different from that in ST0.

Figure 8 shows the ^{13}C CP/MAS NMR spectra of ST83 at 40°C. The assignments were made referring to the spectra of ST0(PMLG), poly(γ-stearyl L-glutamate) (STLG) (corresponding to ST100 with the abbreviation of this work),[23] and *n*-alkanes.[11] The chemical shifts values are listed in Table II. It is known that ^{13}C chemical shifts in the solid state strongly depend on the molecular conformation and crystal structure. Especially, the chemical shift of CO(amide) in polypeptides

Table II. Chemical shifts of ^{13}C CP/MAS NMR spectra

Sample	Temperature	Shift/ppm	α-CH_2		δ-CH_2	int-CH_2		β-CH_2	O-CH_3	C_α	O-CH_2	CO(ester)	CO(amide)
	°C	CH_2	Amorphous	Crystal		Amorphous	Crystal						
ST83	20	14.5		24.8			33.2		51.2	57.0	64.2	172.1	175.9
	40	14.4		24.7	26.2	30.2	32.9		51.1	57.2	64.2	171.8	175.8
	50		22.9		26.2	30.2		32.3		57.3	64.1	171.5	175.5
	60				26.1	30.0		32.1		57.4	64.1	171.5	
	75		22.9		26.2	30.2		32.2	51.2	57.4	64.2	171.5	
ST62	20	14.4	23.0			30.2	32.8		51.5	56.9	64.3	171.6	175.9
	30	14.3	23.0		26.2	30.2	32.4		51.8	57.2	63.9	171.7	175.6
	40	14.2	22.9		26.1	30.1			51.1	57.1	64.1	175.8	175.8
	50				26.2	30.0			51.8	57.2	64.1	175.4	175.4
ST38	20	14.2	23.0		26.2	30.1			51.3	57.1	64.1	171.9	175.8
	40	14.2	22.8		26.1	30.0			51.8	57.2	64.0	171.8	175.8
	50				26.1	29.9			51.1	57.2	64.1	171.8	175.8
	60		22.7		26.1	29.8			50.8	57.3	64.1	171.8	175.8
ST25	20	14.2	22.9		26.2	30.0			51.4	57.0		172.0	175.9
	40		22.8		25.9	29.9			51.1	57.1	63.6	171.9	175.8
	50		22.8		26.0	29.8			51.1	57.2	64.0	172.0	175.9
	60		22.7		26.0	29.9			51.1	57.2	64.2	171.9	175.8
ST0	20								51.6	57.1		172.9	176.0

is sensitive to the main chain conformation as demonstrated by Shoji *et al.*[25] This peak is not strongly affected by side chain structure. As seen in Table II, C_α and CO(amide) chemical shifts are in the ranges of 56.9—57.4 ppm and 175.4—176.0 ppm, respectively, which are characteristic for the right handed α-helical conformation. It is concluded that the copolymers used in this work take the α-helical conformation independent of stearyl group content at least in the temperature range of the measurements.

The chemical shift values of C_δ and CO(ester) are about 26 and 172 ppm, respectively, in all samples, which is very similar to the values for STLG. These results suggest that the conformations of the side chains containing these carbons are independent of D.S. The chemical shifts of int-CH_2 and α-CH_2 for crystalline component are near the values of the corresponding peaks for *n*-alkane in the orthorhombic form rather than the triclinic form. Similar results are obtained from the ^{13}C CP/MAS NMR study of STLG[26] in conflict with X-ray diffraction.[6] Thus, the structure of the side chain crystalline is not influenced by the MLG side chain at least in the scope of this work. For ST38 and ST25, only the peaks of stearyl group in amorphous state are observed in the temperature range of this measurement.

The temperature dependence of the ^{13}C CP/MAS NMR spectra for ST83 are shown in Figure 9. At 20°C, the crystalline peak of int-CH_2 is intense, and the amorphous peak is observed as a shoulder. As the temperature is raised, the intensity of the amorphous peak increases drastically and the crystalline peak rapidly disappears at higher temperature. Similar results are obtained for α-CH_2 peak, suggesting that the α-CH_2 in stearyl group is also concerned with the crystalline part of the side chain. The corresponding peaks for ST62 show similar temperature dependence, although the temperature ranges are lower than that for ST83. For the amorphous peak of int-CH_2, the chemical shift keeps nearly

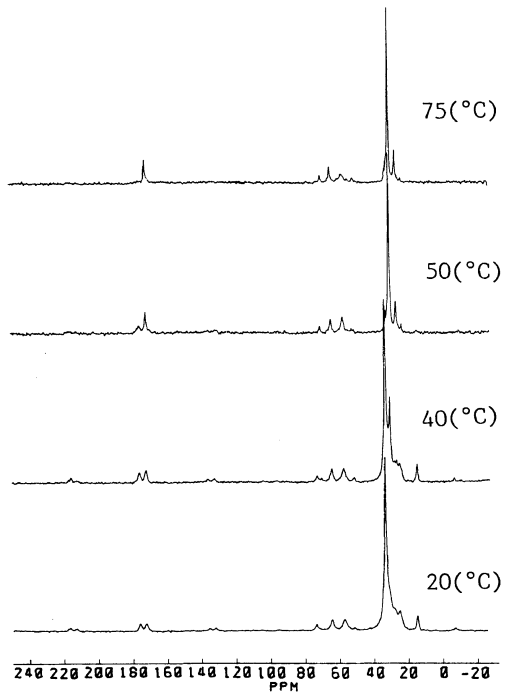

Figure 9. ^{13}C CP/MAS spectra of ST83 at various temperature.

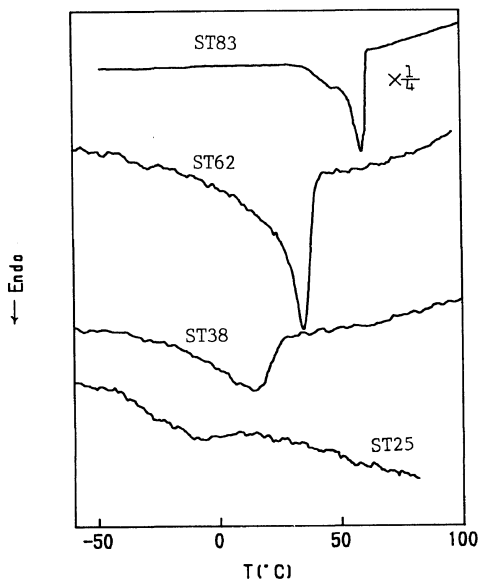

Figure 10. DSC thermogram of ST83, ST62, ST38, and ST25 in the heating process.

constant in all samples independent of MLG content.

Figure 10 shows DSC thermograms in the heating process. Except for ST0 which has no stearyl group, an endothermic peak corresponding to the melting of the side chain crystalline is observed. The peak temperature T_m is listed in Table I. D.S. dependences of T_m and the temperature at which crystalline peaks in CP/MAS spectra disappear have a similar tendency, although there exists 10—20°C difference. These results do not conflict with each other, since the crystalline peak in ^{13}C CP/MAS NMR spectra disappears when there exists considerable gauche conformation of alkyl chain in side chain crystalline. The disagreement may indicate that the molecular motion which induces gauche conformation occurs in the crystalline region at a temperature lower than T_m. It is also considered that the temperature indicated in CP/MAS spectra is the temperature of the bearing air, which may deviate from the sample temperature because of the friction between the air and rotor. That the endothermic peak becomes broader as D.S. decreases may indicate that the size and orderliness of the side chain crystalline tend to decrease with decreasing D.S. For ST83, T_m is close to the temperature range of the sudden decrease in ESR correlation time, supporting that such decrease is caused by melting of the side chain crystalline. Other samples do not show such abrupt decrease in ESR correlation times near the melting point of the side chain crystalline. In those samples, crystallinity is low and the amorphous region where spin-probes exist is wide enough not to be influenced by the crystalline region.

Figure 11 shows the scalar decoupled ^{13}C NMR spectra of ST62. Some peaks can be identified even though no technique to remove the dipole interaction is employed. These peaks appear therefore due to averaging of dipole interactions by fast motion. The assignment of peaks are listed in Table III. Only the peaks that arise from stearyl group in the amorphous state are identified, indicating stearyl groups in amorphous state are especially mobile, differing very much from other parts of the side chain. The ESR results suggest that the motional state in copolymers differs much from that in ST0(PMLG), and that spin-probe exists in the amorphous region consisted of stearyl groups. The consideration agrees with the

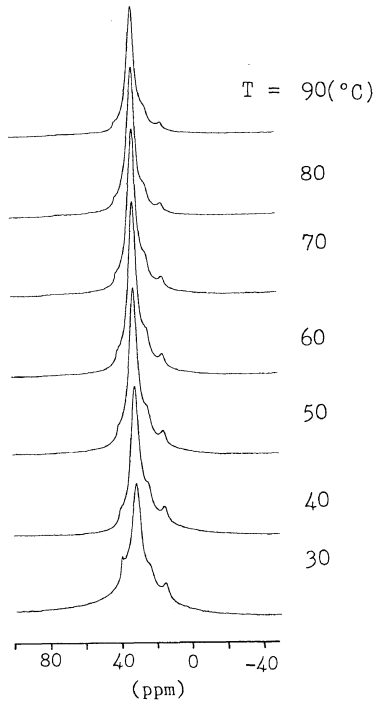

Figure 11. ^{13}C NMR spectra with scalar decoupling of ST62 at various temperature.

Table III. Chemical shifts of scalar decoupled ^{13}C NMR spectra

Sample	Temperature	Peaks/ppm	
	°C	CH_3	int-CH_2 (amorphous)
ST62	30	14.9	31.0
	40	14.6	30.8
	50	14.6	31.3
	60	14.9	30.8
	70	14.7	30.8
	80	14.8	31.1
	90	14.8	31.1

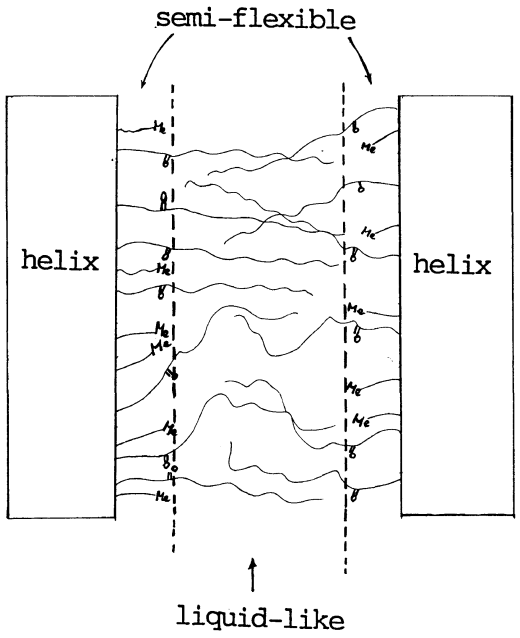

Figure 12. Schematic representation of the motional state of the side chain region.

results for polyethylene.[12] Kusumoto *et al.* reported that spin-probe is not immersed in the crystalline region and reflects the motional state of the amorphous region. D.S. dependence of the motional state of copolymers is not so remarkable in the higher temperature region, indicating that mobility of the amorphous region is not affected by the MLG side chain. In the case of ST83, the amorphous region is so small that the spin-probe is constrained by the crystalline region, because of high crystallinity or increase in crystalline size as shown by the results of ^{13}C CP/MAS and DSC. Based on these results, the structure of the copolymer is schematically shown in Figure 12. At higher temperature, side chain region is classified as two parts by mobility, a semi-flexible part (inner-part) and liquid-like part (amorphous part of the stearyl group). At a lower temperature than T_m, paraffin-like crystallines are formed partially in the liquid-like part. The mobility of the liquid like part has small D.S. dependence, indicating weak interactions between the two parts. This feature may be important for the formation of the side chain crystalline, since it allows for the stearyl group to take a conformation not restricted by the other part and behave as paraffin molecule as pointed out by Watanabe *et al.*[4] The extremely high mobility of the liquid like part which is not restricted by the semi-flexible part at higher temperature is considered to be important for reorientation of the main chain to form liquid-crystals.

CONCLUSION

The side chain region of the copolymer of MLG and STLG in the lower temperature region than T_m can be divided to three parts: an inner part composed of MLG side chains and inner portion of the STLG side chains, an amorphous part of stearyl groups, and a crystalline part of stearyl groups. The motion of inner part is constrained and relatively slow. Spin-probes mainly exist in the amorphous part, and do not exist in the crystalline part. The motion of spin-probes is constrained by the crystalline part when crystallinity becomes high. In the higher temperature than T_m, even small D.S. makes the mobility of amorphous part extremely high and no remarkable dependence on D.S. is observed.

Acknowledgments. The authors wish to express their gratitude to Dr. S. Shimokawa, Mr. F. Ishii, and Dr. T. Hiraoki of Hokkaido University for the valuable advice and fruitful discussion. They are also grateful to Mr. E. Yamada of the NMR laboratory in Hokkaido University for recording the NMR spectra, and finally they express their appreciation to the members of their laboratory for their assistance and encouragement.

REFERENCES

1. K. Hikichi, K. Saito, M. Kaneko, and J. Furuichi, *J. Phys. Soc. Jpn.*, **19**, 557 (1964).

2. A. Tsutsumi, K. Hikichi, T. Takahashi, Y. Yamashita, M. Matsushima, M. Kanke, and M. Kaneko, *J. Macromol. Sci., Phys.*, **B8**, 413 (1973).
3. Y. Yamashita, A. Tsutsumi, K. Hikichi, and M. Kaneko, *Polym. J.*, **8**, 114 (1975).
4. J. Watanabe, H. Ono, I. Uematsu, and A. Abe, *Macromolecules*, **18**, 2141 (1985).
5. J. Watanabe, Y. Fukuda, R. Gehani, and I. Uematsu, *Macromolecules*, **17**, 1004 (1984).
6. J. Watanabe, M. Goto, and T. Nagase, *Macromolecules*, **20**, 298 (1987).
7. L. J. Berliner, Ed., "Spin labeling," Theory and Applications, Academic Press, New York, N.Y., 1976.
8. P. Meurisse, C. Friedrich, M. Dvolaitzky, F. Laupretre, C. Nöel, and L. Monnerie, *Macromolecules*, **17**, 72 (1984).
9. F. Laupretre and L. Monnerie, *Macromolecules*, **17**, 1397 (1984).
10. J. Schaefer, E. O. Stejskal, and R. Buchdhl, *Macromolecules*, **10**, 384 (1984).
11. T. Sorita, T. Yamanobe, T. Komoto, and I. Ando, *Makromol. Chem. Rapid Commun.*, **5**, 675 (1984).
12. N. Kusumoto, in "Molecular Motion in Polymer by ESR," R. F. Boyer and S. E. Keinath, Ed., Harwood, Chur, 1980.
13. G. L. Slonimski, A. A. Askadskii, and A. I. Kitagorodskii, *Vyskomol. Soyedin., Ser. A*, **12**, 494 (1973).
14. J. H. Freed, *J. Chem. Phys.*, **41**, 2077 (1964).
15. A. Capiomont, B. Chion, J. Lajzerowicz-Bonneteau, and H. Lemaire, *J. Chem. Phys.*, **60**, 2530 (1974).
16. A. L. Kovarskii, A. M. Vasserman, and A. L. Buchachenko, *Vyskomol. Soedin., Ser. A*, **13**, 1647 (1971).
17. S. A. Goldman, G. V. Bruno, and J. H. Freed, *J. Chem. Phys.*, **76**, 1858 (1972).
18. A. Tsutsumi, *Jpn. J. Appl. Phys.*, **9**, 1125 (1970).
19. Y. Yamashita, A. Tsutsumi, K. Hikichi, and M. Kaneko, *Polym. J.*, **8**, 114 (1976).
20. A. Tsutsumi, K. Hikichi, T. Takahashi, Y. Yamashita, N. Matsushima, M. Kanke, and M. Kaneko, *J. Macromol. Sci. Phys.*, **B8**, 413 (1973).
21. G. V. Bruno, J. H. Freed, and C. F. Plonaszek, *J. Chem. Phys.*, **75**, 3385 (1971).
22. A. Tsutsumi, K. Yoshikawa, and T. Hideshima, *Rep. Prog. Polym. Phys. Jpn.*, **28**, 505, (1985).
23. (a) T. Kajiyama, M. Kuroishi, and M. Takayanagi, *J. Macromol. Sci.-Phys.*, **B11**, 121 (1975). (b) T. Kajiyama, M. Kuroishi, and M. Takayanagi, *J. Macromol. Sci.-Phys.*, **B11**, 195 (1975).
24. M. Tsukahara, T. Yamanobe, T. Komoto, J. Watanabe, and I. Ando, *J. Mol. Struct.*, **159**, 345 (1987).
25. A. Shoji, T. Ozaki, H. Saito, R. Tabeta, and I. Ando, *Macromolecules*, **17**, 1472 (1984).
26. T. Yamanobe, M. Tsukahara, T. Komoto, J. Watanabe, I. Ando, I. Uematsu, K. Deguchi, T. Fujito, and M. Imanari, *Macromolecules*, **21**, 48 (1988).